Atomistic simulation of the interface structure of Si nanocrystals embedded in amorphous silica

Flyura Djurabekova and Kai Nordlund*
Department of Physics, Helsinki Institute of Physics, University of Helsinki, P.O. Box 43, Helsinki FIN-00014, Finland
(Received 21 December 2007; revised manuscript received 11 February 2008; published 14 March 2008)

An efficient means to obtain light emission from a silicon-based material would enable integrating both optical and electronic functionalities on the same silicon chips. The long radiative lifetimes have until recently obstructed efficient light emission from Si. A nanocrystalline approach has opened up a prospect for silicon in the optoelectronics application field. However, the structure of the nanocrystal-matrix interface, which appears to be important for the light emission, remains unclear. In the present work, by means of molecular dynamics atomistic models, small nc-Si embedded into defect-free a-SiO_2 are constructed using two different classical interatomic potentials. The models allow analysis of the defects at the interface which may serve as radiative and nonradiative recombination centers for excitons formed in nc's and, thus, be responsible for the optical properties of the structure. We analyzed the interface structures after a series of high-temperature annealing runs and subsequent relaxation at room temperature. The results show that the nc-Si/SiO_2 interface is organized by means of a thin suboxide layer (SiO_{2-x}), which contains a considerable amount of undercoordinated defects as well. We also observed the spontaneous formation of silanone bonds (Si=O), frequently discussed in the literature to be centers with an important role on the optical properties of the nc structures.

DOI: 10.1103/PhysRevB.77.115325 PACS number(s): 81.07.Ta, 78.67.Bf, 79.60.Jv

I. INTRODUCTION

The normally inefficient light-emitting properties of silicon were recently significantly enhanced within a nanocrystalline (nc) approach. Silicon nanocrystals showed a visible luminescence, interpreted to be a result of a quantum confinement effect.[1,2] The wavelength of emitted light was also found to depend strongly on the size of the nc-Si: the smaller the nanocrystals emitted, the shorter the lightwaves with stronger intensity. Since such nanocrystals can be manufactured with ion implanters, a tool commonly present in industrial wafer manufacturing lines, this has opened up a promising avenue for using low-cost silicon chips for optoelectronics.

Already in 1990, Canham *et al.*[1] found a strong photoluminescence (PL) in po-Si, where the length and intensity of the light could be controlled by the porosity of silicon. Unfortunately, the functionality of po-Si was limited by instability of the optical properties, which are sensitive to the external ambients. For instance, PL degrades quickly under simultaneous exposure to the oxygen and light.[3] In 2000, Pavesi *et al.*[4] indicated that stable light amplification can be achieved with nc-Si embedded into a-SiO_2. A year later, Khriachtchev *et al.*[5] showed that the amplified pulses in these systems can be very short, which is very important for fast operation of optical devices. These observations have stimulated a generation of research activities in this field. The main interest has been on obtaining better understanding of the physical processes in order to control the optical properties and increase the optical gain in the structures.[6] Maximization of the free carrier confinement and a significant decrease of the radiative lifetime, responsible for the PL of small nc-Si which is in the visible range, have been fairly well explained within the quantum confinement theory.[7,8] However, the superior properties of embedded nc-Si compared to po-Si or freestanding nc-Si are still not clear.[9]

Regarding the embedded nanocrystals, the significance of the nc-Si/a-SiO_2 interface on the optical properties is intensively debated.[6,9] It has already been shown that the oxidation of po-Si causes a large PL redshift as a result of stabilized Si=O surface states in the energy band gap, where an electron or exciton can be trapped, especially for the small-size nanocrystallites (<3 nm).[10] On the other hand, the sharpness of the Si/SiO_2 interface, as well as its stability with respect to external agents, stabilizes the PL phenomenon. In addition, the oxygen and related defect states at the interface can serve as radiative recombination centers for carriers and make a significant effect on the optical properties of the system. This makes the embedded structures highly promising for practical application[9,11] and also emphasizes the importance of theoretical understanding of the nature of the interface.

Thanks to its wide technological application, the planar Si/SiO_2 system is one of the most studied interfaces. Nonetheless, due to the complexity of the amorphous network, the interface between crystalline silicon and amorphous silicon dioxide has lacked a realistic theoretical model. The fairly well-understood defects which may appear during the formation of the interface such as stretched Si—Si bonds and dangling bonds are not included in the existing nc interface models, even though they are important as they introduce broad states into the band gap.[12]

Previous theoretical models of Si/SiO_2 and nc-Si/SiO_2 interfaces form basically two general groups. Models employing density functional theory (DFT) methods are able to treat only quite small systems with a very limited number of atoms in the nanocrystal due to the heavy computational cost.[9,13,14] Moreover, the DFT models assume an ordered structure of SiO_2, corresponding to α- or β-quartz supercells, instead of a random amorphous network. Models employing Monte Carlo (MC) bond-switch algorithms using the Keating potential can treat realistic-sized nanocrystals (with diameters of ~2–5 nm).[15,16] However, in this MC algorithm, the formation of dangling bonds is prohibited, as the algorithm forces all atoms to have an ideal coordination environment.

TABLE I. Number of coordination defects and suboxides in the a-SiO_2 cubic cell with an initial side length of 6 nm cooled by MD with periodic boundaries. The structures are obtained from the randomized distribution of Si and O atoms as a function of the cooling rate. Results are given for the potentials of Watanabe (Ref. 19) and Ohta (Ref. 18).

Rate (K/fs)	Undercoordinated (%)		Overcoordinated (%)		SiO_x (%)	
	Watanabe	Ohta	Watanabe	Ohta	Watanabe	Ohta
1	13	12.8	0.5	5.7	5.7	0.3
0.5	10.3	12	0.4	5	4.2	0.2
0.3	9.2	10.5	0.3	5	3.8	0.2
0.2	8.6	10.2	0.3	4.6	3.8	0.1
0.1	7	8.6	0.3	4	2.6	0.02
0.05	6.1	7	0.2	3	2.5	0.05
0.03	5.7	6	0.14	2.6	1.8	0.02
0.02	5.5	5	0.12	2.5	1.9	0.05
0.01	4.5		0.12		1.8	

In spite of the rigid assumptions done in these models, they show that the nc-Si/SiO_2 interface behaves differently from Si/SiO_2, having an extended transition region, which affects optical properties of the structure as well.[9]

In the present work, we utilize computationally efficient classical interatomic potentials and molecular dynamics (MD)[17] simulation to approach the experimental conditions by creating realistic-sized atomistic model of the nc-Si embedded into an amorphous silica matrix. We employ interatomic potentials that are able to treat both pure Si and SiO_2 in the same functional form.[18,19] In this approach, it is possible to carry out high-temperature annealings to optimize the interface structure, without any built-in assumptions of the bonding or matrix structures or atom movement paths.

II. METHODS

A. Atomistic models of amorphous silica

As a host matrix which has a peculiar amorphous structure, a silica cell requires a prior thorough preparation procedure. In our simulations, we are applying the interatomic potentials of Watanabe[19,20] and Ohta,[18] which were developed to describe the Si-O mixed systems on the base of the classical Stillinger–Weber potential. These potentials have the advantage that they can describe in addition to the ideal bonding environment also coordination defects.

To test how well the potentials can describe a-SiO_2 without any built assumptions, we carried out MD simulations of the annealing of silica starting from atom positions distributed initially completely randomly, except that the minimum interatomic distance was restricted to be no less than 1.9 Å to prevent unrealistically high interaction energies between both Si-O and Si-Si atoms.

Having started with the number of silicon and oxygen atoms (as ratio 1:2) and a cell volume corresponding to the atomic density of a-SiO_2, we found that simple MD cooling of the system to the room temperature indeed results in a random silica network. The quality of the structure strongly depends on the cooling rate. In quartz as well as vitreous silica, the ideal coordination state is that all Si atoms have four bonds to O and all O atoms have two bonds to Si. Thus, any deviations from this coordination state can be considered as defects in the random silica network.[21]

An additional number of subsequent annealing runs, concluded by a pressure control MD run to zero pressure, allowed improving the quality of the network by decreasing the number of under- and overcoordinated atoms. Table I displays the dependence of the quality of a silica cell (the number of coordination defects and suboxide atoms) as a function of the cooling rate. We use the denotation "suboxide atoms" for atoms with the same coordination number as in ideal silica (four for Si and two for O) that have bonds to both Si and O atoms.

Although even the lowest cooling rates did not produce a silica cell with no coordination defects in it, the table shows clearly that the quality of the structure steadily improves with decreasing cooling rate. The smallest cooling rate used in these calculations gives less than 5% of defects and less than 2% of suboxides. Thus, it is reasonable to assume that on typical experimental cooling rates (much lower than those accessible to MD simulations), a virtually defect-free a-SiO_2 would be obtained.

The higher probability of suboxide bond formation with the Watanabe potential can be explained by the smaller difference of average cohesive energy per atom between a pure silica and a pure silicon material (see Table II). For the Ohta potential, the creation of extra bond to a correctly coordi-

TABLE II. The average cohesive energies per atom $<E_c>$ in pure silicon and silica according to the potentials of Watanabe and Ohta. Also given is the experimental value of $<E_c>$ for silica (Ref. 23).

		a-SiO_2		
	c-Si	Watanabe	Ohta	Expt.
$<E_c>$ (eV/atom)	4.33	5.26	9.7	6.42

nated atom requires a lower-energy penalty compared to the penalty required to substitute a neighbor atom with an atom of opposite type. This is because the Ohta potential strongly overestimates the Si-O binding energy (see Table II). This leads to the higher number of overcoordinated defects in the Ohta potential.

The value of cohesive energy obtained with the Watanabe potential is closer to the experimental value (last column in Table II). Due to this, in the remainder of the paper, we only present results obtained with the Watanabe potential, since both Si and SiO_2 are present at the interface, and the high probability of formation of overcoordinated defects may mislead the interface analysis. In a previous study, we constructed 2.4 nm nc-Si inserted in smaller (4 nm of a side) SiO_2 cells with both the potential of Watanabe and Ohta. There we found with the Ohta potential 14.3%, 3.8%, and 11% of the undercoordinated, overcoordinated, and suboxide atoms at the interface (given as fractions of all interface atoms), respectively, whereas the Watanabe potential gave 10.5%, 1.6%, and 12.8% for the same quantities. While the main results were qualitatively the same for both potentials, the main quantitative difference was a higher number of overcoordinated interface defects and lower number of suboxide atoms in the Ohta potential.[22]

Since obtaining fully coordination-defect-free silica was not possible by the MD method, we also used the Wooten-Winer-Weaire (WWW) technique for constructing a perfect random network.[24] To obtain a random silica network, we used the WWW Monte Carlo code BOMC.[25] In this approach, the network is evolving by bond-switch Monte Carlo moves which are accepted or not according to a rigid Keating potential.[25] As a second step, we relaxed the structure obtained from the BOMC code by MD to room temperature and zero pressure for 75 ps using the Watanabe potential. This rearranged the positions of atoms to be compatible with the potential used for the insertion of the nanocrystal.

We compared the pair correlation functions and Si—O—Si bond-angle distributions for all the networks we had obtained to the published experimental neutron-diffraction data by Susman *et al.*[26] and the Mozzi–Warren diffraction results[27] [Figs. 1(a) and 1(b)]. Dashed lines correspond to the MD annealed silica cells with the Ohta potential, and dotted lines correspond to the same cells annealed with the Watanabe potential. Rarefied dotted lines stand for the MC cell relaxed with the Watanabe potential and solid lines are experiment. The good agreement for the pair correlation function curves proves that the obtained networks are realistic in structure. The second graph shows that the MD annealed cells have also bond-angle distribution closer to the real distribution than the ideal MC network. Unfortunately, the significant number of coordination defects that remained in the MD cell limits the application of annealed networks for our study. For this reason, we chose the MC silica network relaxed with the Watanabe potential. Bonding analysis showed that after relaxation, this network generally remains defect-free except for a small fraction ($\lesssim$0.1% of all atoms) of coordination defects.

B. nc-Si inserted into *a*-SiO_2 cell

We constructed the atomistic model of a nc in an amorphous matrix, as depicted schematically in Fig. 2. A ball of

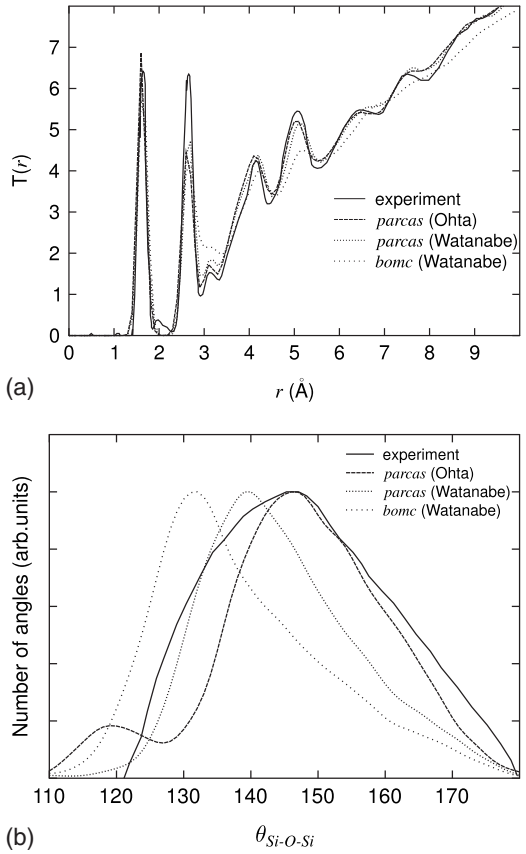

FIG. 1. Pair correlation function in the form of weighted $T(r)$ (Ref. 26) (a) and bond-angle function $\theta_{\mathrm{Si—O—Si}}$ for the *a*-SiO_2 cells. The data were obtained by cooling the randomized mixture of Si and O atoms by MD (PARCAS) with the potentials of Watanabe (dashed lines) and Ohta (dotted lines), as well as by MC switch-bond method (BOMC) (Ref. 25) with subsequent relaxation with the Watanabe potential (black dashed lines). The solid lines represent the experimental curves from Ref. 26 in (a) and the Mozzi–Warren diffraction result (Ref. 27) in (b).

the given diameter initially cut out from a perfect crystalline Si cubic cell (nc-Si) was inserted into the cubic *a*-SiO_2 cell with a sidelength of 6 nm obtained by the above-described technique. The nc-Si replaced a hole of the same diameter cut out in the center of the silica cell. Prior to insertion, we slightly compressed the nc-Si over its volume (for 3 Å less in diameter) in order to avoid the formation of unreasonably short bonds due to the size equality of a nc-Si and a hole. A following short MD pressure relaxation run released the compressive stresses, restoring the nc into its initial state, but allowing no short atomic distances at the interface. In this way, we prepared the nc-Si; of three different diameters of 1.3, 2.4, and 3.6 nm with 71, 329, and 1226 atoms in each, respectively, to be able to follow the size effect on the defect structure of the interface.

The preparation of the nc-Si/SiO_2 structure was performed as a series of annealing runs combined with pressure control. A statistical variation was provided by random shifts of the insertion position of the nc, i.e., the same spherically cut nc surface facing different parts of the silica matrix, forming different interfaces.

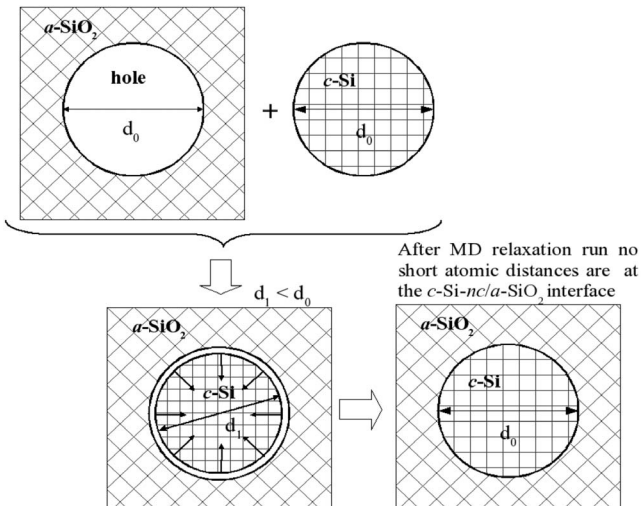

FIG. 2. Method for insertion of the crystalline ball into the hole of the same radius inside of amorphous matrix. The crystalline ball is cut out of a perfect crystalline cubic cell of bigger size than the required diameter of nanocrystal.

A series of three different annealing runs were applied between the temperatures, (i) 1100 and 300 K, (ii) 1400 and 300 K, and (iii) 1600 and 300 K, with subsequent decrease of maximum temperatures, in order to find a reasonably low-energy interface structure. A last pressure control run carried out after every annealing mode at a constant temperature of 300 K run was used to release the strain due to temperature ramping procedures. All the processes have been monitored by the value of the average total energy per atom. The difference of this quantity in the final structures for different interfaces never exceeded 0.02 eV/atom for either potential. The small difference between different cells showed that the system was overall well converged in energy. However, the number of the interface atoms is much smaller than the number of atoms in the entire system. Hence, the actual number of defects in the interface region is fairly small and thus cannot significantly affect the averaged quantities.

The analysis of the interface in case of the smallest nc-Si was confounded by the fact that the small nc-Si (1.3 nm in diameter) in our simulations almost lost the crystalline structure already at the lowest annealing mode (i). A similar feature of the small nc's was reported in an MC study by Hadjisavvas and Kelires.[16] The bigger nc-Si kept the crystallinity also after annealing mode (iii), making the interface analysis more reliable. Atomic models of nc-Si inserted into silica of 1.3, 2.4, and 3.6 nm in diameters are depicted in Figs. 2(a)–2(c), respectively. The latter shows a clear interface region, which can be analyzed with respect to the nature of defects.

III. RESULTS AND DISCUSSION

As discussed in the previous section, the analysis of the interface formed by small nc-Si (<2 nm in diameter) with a-SiO_2 is quite confounding. Hence, we analyzed nc's of the larger sizes of 2.4 and 3.6 nm in detail, examining ten different interfaces in each case for nc's to obtain statistics. Plotting the potential energy for an entire cell per atom as a radial distribution [Fig. 4(a)], one can see that all the defects are clearly located in a narrow area around the interface, and thus, the width of the interface region can be determined from these plots. Quantitatively speaking, the width was determined as the difference between two radii which restrict the area where the concentration of coordination defects was significant in comparison with the rest of a nc and a host matrix. The additional plot of the radial distribution of coordination defects, zoomed in to show the interface region for the same structure, shown in Fig. 4(b), helps in identifying the nature of the defects. The most favorable coordination defect formed at the interface is an undercoordinated defect with one dangling bond; this result is well in line with the defect model for planar Si/SiO_2 interfaces discussed in Ref. 12 and also in very good agreement with DFT studies of planar interfaces (see, for example, Ref. 28).

The suboxide atoms are not visible in Fig. 3(b) since they have fourfold bonds, but they are associated with a difference in the total energy. This is reflected as a much larger number of dots in the interface "cloud" in Fig. 4(a) (potential energy) compared with Fig. 4(b) (coordination defects). We analyzed the presence of suboxide atoms using bonding neighborhood analysis. Although the particular nature of suboxides is difficult to determine, we found that the most common replacement of only one atom by the atom of different types had happened, while a smaller number of atoms had 2 atoms replaced by atoms of different types. We have also checked the possibility for both Si and O atoms (both missing one bond) to appear close to each other. This combination may result in the formation of a silanone Si=O bond, known as a radiactive recombination center for free carriers generated in the nc in favor of a defect-assisted recombination mechanism for the PL in the nc structures.[6,14] In a DFT study, Luppi and Ossicini[14] showed that the strong reduction in the energy gap causing a huge redshift after oxygen exposure of silicon nanoparticles can be explained by the presence of a silanone bond (an oxygen atom double bonded to a Si) at the surface of nanoparticle. However, according to their model, a number of Si=O bonds bigger than one did not enhance the effect significantly. According to our observations, the silanone bonds can be spontaneously formed during the annealing process of embedded nc's into silica matrix. Almost at each investigated interface, at least one silanone bond was found. The bigger area of the interface (nc of 3.6 nm) gave better statistics, but we could not observe a clear size dependence of the effect due to the poor statistics.

In Table III, we summarized our results on the interface analysis for 2.4 (upper part) and 3.6 (lower part) nm nc-Si, respectively, versus the annealing temperature. It includes the width of the interface, coordination defects, and suboxides as a percent fraction relative to the entire number of interface atoms. We also calculated the excess interface energies of the system as

$$\gamma = 1/(4\pi r_{\mathrm{nc}}^2)\{E_{tot}^{\mathrm{Sinc}} - [E^{c,\mathrm{Si}}N_{\mathrm{Si}}^{\mathrm{nc}} + (E_{\mathrm{Si}}^{c,\mathrm{SiO_2}}N_{\mathrm{Si}} + E_{\mathrm{O}}^{c,\mathrm{SiO_2}}N_{\mathrm{O}})]\}.$$

Here, $E_{tot}^{\text{nc-Si}}$ is the total potential energy in the cell with an embedded nc, $E^{c,\mathrm{Si}}$ is the average cohesive energy per atom

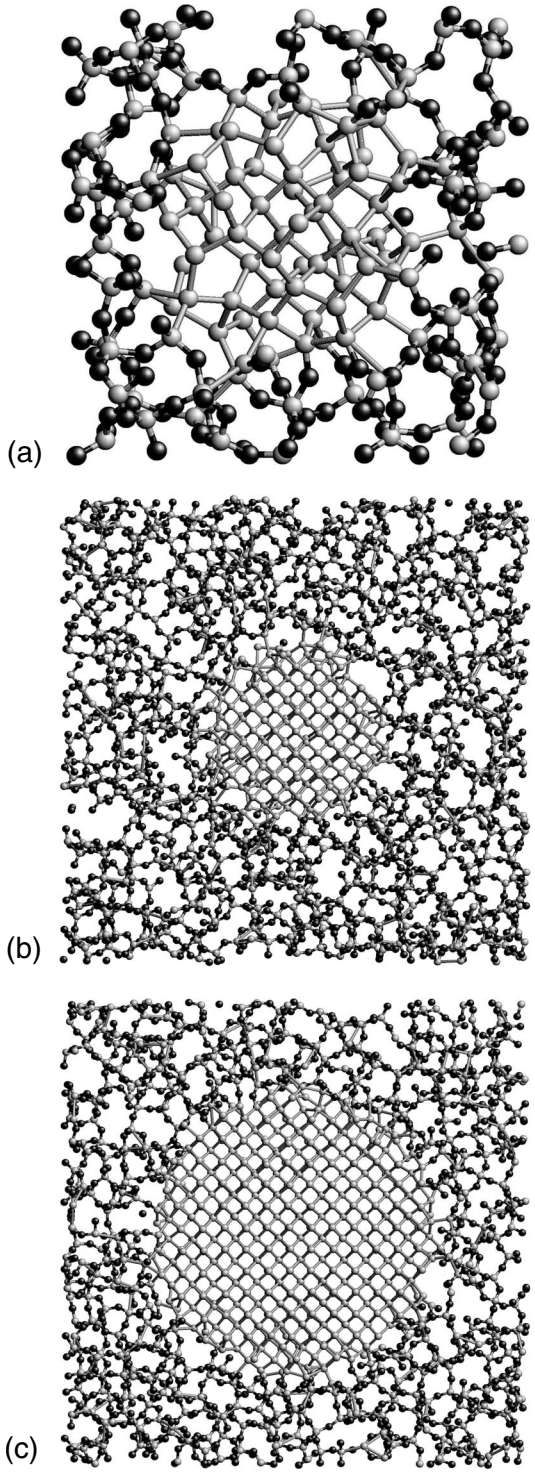

FIG. 3. Atomistic model of nc-Si [(a) 1.3 nm, (b) 2.4 nm, and (c) 3.6 nm] embedded into amorphous silica obtained by MD after series of annealing runs; gray and black circles are silicon and oxygen atoms, respectively.

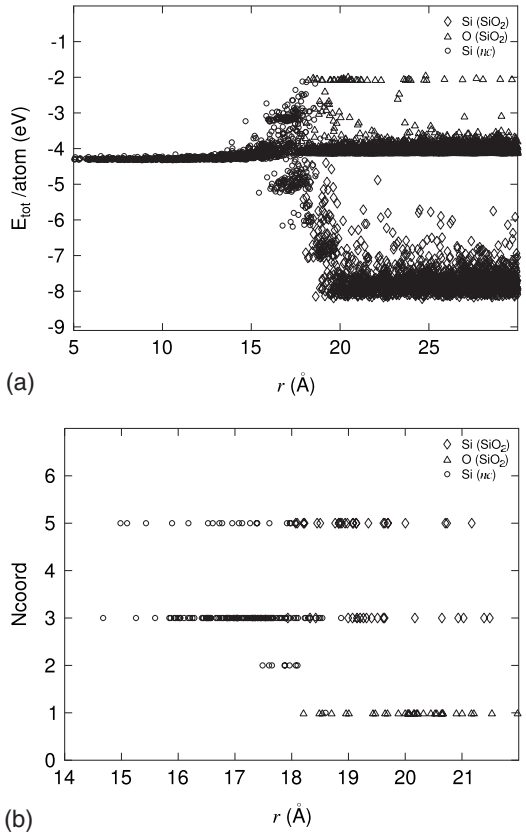

FIG. 4. Radial distributions of the (a) total energy per atom and (b) coordination defects for the nc-Si/SiO_2 obtained by annealing of cell with 3.6 nm nc-Si at 1400 K. The Si atoms of nc-Si (○) are shown differently from Si of a-SiO_2 (◇). △ is used to represent O atoms. Note that the r scale in (b) is focused on the interface region.

in pure silicon, $E_{\mathrm{Si/O}}^{c,\mathrm{SiO_2}}$ are the average cohesive energies per Si/O atom in the pure silica cell, $N_{\mathrm{Si/O}}$ are the numbers of Si/O atoms in the silica part of the cell with an embedded nc, $N_{\mathrm{Si}}^{\mathrm{nc}}$ is the number of Si atoms in the nc, and r_{nc} is a radius of the nc. Note that in this definition of an interface energy, the surface energies are not substracted out, which is consistent with previous usage in the field.[13]

The excess interfacial energies obtained in our calculations are shown in the last column. All the values compare well with the recent DFT value of 0.093 eV/Å^2.[13] We did not find a clear dependence of these values on the size of the nc (the small discrepancies between γ for both sizes at the

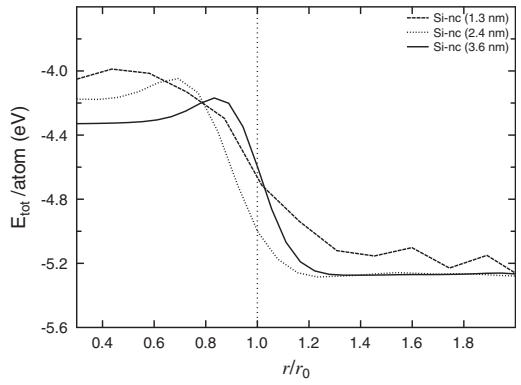

FIG. 5. Radial distributions of the potential energy per atom as a function of the distance from the center of the cluster for cells which contain 1.3 nm (dotted line), 2.4 nm (dashed line), and 3.6 nm (solid line) nc-Si. The average is over all atoms in the ten simulation cells of the same-sized nanocrystal.

TABLE III. nc-Si/a-SiO_2 interface defects as the percentage of the total amount of interface atoms, the mean width of the interface, and corresponding interfacial energies for both 2.4 nm (upper part) and 3.6 nm (lower part) nc-Si. The error bars are the standard error of the mean.

T_a (K)	Undercoordinated (%)	Overcoordinated (%)	Suboxide atoms (%)	Δr_{IF} (Å)	γ (eV/Å^2)
1100	9.2 ± 0.3	1.8 ± 0.2	11.1 ± 0.4	9.9 ± 0.8	0.087 ± 0.002
1400	8.4 ± 0.6	1.6 ± 0.2	10.2 ± 0.5	9.9 ± 0.8	0.076 ± 0.003
1600	8.3 ± 0.6	1.4 ± 0.1	11.8 ± 0.9	9.3 ± 0.9	0.072 ± 0.002
1100	11.1 ± 0.5	2.1 ± 0.1	9.9 ± 0.7	7.3 ± 0.4	0.094 ± 0.003
1400	10.5 ± 0.5	2.3 ± 0.2	11.1 ± 0.7	6.9 ± 0.2	0.083 ± 0.002
1600	9.6 ± 0.3	2.2 ± 0.1	11.3 ± 0.6	7.0 ± 0.2	0.077 ± 0.002

same annealing temperatures are within the statistical error). At the same time, we observed a certain decrease of γ for both nc's with elevating the annealing temperature.

The width of interfaces in all cases agrees excellently with the experimentally estimated value of 0.8 nm for the planar Si/SiO_2 interface.[29] Our calculations of single nanocrystal size show that the bigger size of the nc-Si stabilizes the interface, constraining it in a thinner region. To understand this observation, we analyzed the average potential energy per atom as a function of radius. The results are shown in Fig. 5, where the energy in each cell is displayed relative to the radius of original nc. The interface affects much stronger the outer parts of the silicon crystal structure. The distortion of the crystal structure grows severer with decreasing nc diameter, since the larger crystals have an internal cohesion which can better counteract the stress from the interface. The shift of the maximum of potential energy inside of the nc-Si shows that the width of the interface grows with decreasing of nc diameter. The potential energy of the smallest nc remains much higher than the potential energy of pure silicon up to its center and corresponds to the value of amorphous silicon.[30] Note also that the areas under the curves corresponding to the 2.4 and 3.6 nm nc's are almost equal, which confirms that the interfacial energies for both sizes would not differ significantly.

Our observation on the fair amount of dangling bonds (which mostly serve as centers for nonradiative recombination of excitons) present at the nc-Si/SiO_2 interface (Table III) is well in line with experimental evidence of PL enhancement in samples which contain nc-Si embedded into the silica matrix found after passivation of the samples in different annealing ambients. The increase of PL intensity was attributed to the elimination of nonradiative recombination centers in the SiO_2 matrix and in the nc-Si/SiO_2 interface.[31,32]

IV. CONCLUSIONS

By means of MD methods, we have constructed atomistic models of Si nanocrystals of three different sizes embedded into a-SiO_2. The interfaces were prepared applying three different annealing temperatures. The results showed that the smallest nanocrystals with sizes of <2 nm lose the crystalline structure already at the lowest (1100 K) annealing temperature. The interface analysis of bigger nc's (2.4 and 3.6 nm in diameter) showed that the interface mainly affects the outer part of Si crystallites and that the smaller nc has a lower interfacial energy. The most common coordination defects created in the interface are Si atoms with one dangling bond. The relative number of coordination defects almost does not vary with the size and never exceeds $\sim 10\%$ of the total number of interface atoms. We also found the fair amount of suboxide atoms (right-coordinated atoms with both Si and O nearest neighbor atoms) which was close to the number of dangling bonds at the interface. The ratio between coordination defects and suboxides is slightly changing with increasing annealing temperature: most likely, some of the coordination defects eventually turn into suboxides. The analysis also revealed the presence of Si=O ("silanone") bonds, which are known to be important for the optical properties of nc-Si/SiO_2 structures. The width of the interfaces was shown to agree well with an experimental value of 0.8 nm obtained for a distribution of nc sizes. From our simulations, we were able to compare how the interface width changes with the precise nc size and showed that the bigger nanocrystal had a thinner interface region.

ACKNOWLEDGMENTS

We thank J. Samela for useful discussions and S. von Alfthan for providing us with the "BOMC" computer code. This work was performed within the Finnish Centre of Excellence in Computational Molecular Science (CMS), financed by The Academy of Finland and the University of Helsinki, and also financed by Academy projects OPNA and CONADEP. Grants of computer time from the Center for Scientific Computing in Espoo, Finland, are gratefully acknowledged.

*flyura.djurabekova@helsinki.fi

[1] L. T. Canham, Appl. Phys. Lett. **57**, 1046 (1990).
[2] C. Pickering, L. T. Canham, and D. Brumhead, Appl. Surf. Sci. **63**, 22 (1993).
[3] M. A. Tischler, R. T. Collins, J. H. Stathis, and J. C. Tsang, Appl. Phys. Lett. **60**, 639 (1992).
[4] L. Pavesi, L. D. Negro, C. Mazzoleni, G. Franzo, and F. Priolo, Nature (London) **408**, 440 (2000).
[5] L. Khriachtchev, M. Rasanen, S. Novikov, and J. Sinkkonen, Appl. Phys. Lett. **79**, 1249 (2001).
[6] L. Pavesi and G. Guillot, in *Optical Interconnects: The Silicon Approach*, edited by W. Rhodes (Springer, Berlin, 2006).
[7] J. P. Proot, C. Delerue, and G. Allan, Appl. Phys. Lett. **61**, 1948 (1992).
[8] L.-W. Wang and A. Zunger, J. Phys. Chem. **98**, 2158 (1994).
[9] N. Daldosso, M. Luppi, S. Ossicini, E. Degoli, R. Magri, G. Dalba, P. Fornasini, R. Grisenti, F. Rocca, L. Pavesi, S. Boninelli, F. Priolo, C. Spinella, and F. Iacona, Phys. Rev. B **68**, 085327 (2003).
[10] M. V. Wolkin, J. Jorne, P. M. Fauchet, G. Allan, and C. Delerue, Phys. Rev. Lett. **82**, 197 (1999).
[11] L. D. Negro, M. Cazzanelli, N. Daldosso, Z. Gaburro, L. Pavesi, F. Priolo, D. Pacifici, G. Franzò, and F. Iacona, Physica E (Amsterdam) **16**, 297 (2003).
[12] W. Fussel, M. Schmidt, H. Angermann, G. Mende, and H. Flientner, Nucl. Instrum. Methods Phys. Res. A **377**, 177 (1996).
[13] P. Kroll and H. J. Schulte, in *Group IV Semiconductor Nanostructures–2006*, edited by L. Tsybeskov *et al.*, MRS Symposia Proceedings No. 958, L07-16 (Materials Research Society, Pittsburgh, 2007).
[14] M. Luppi and S. Ossicini, Phys. Rev. B **71**, 035340 (2005).
[15] E. Lioudakis, A. Othonos, G. C. Hadjisavvas, P. C. Kelires, and A. G. Nassiopoulou, Physica E (Amsterdam) **38**, 128 (2007).
[16] G. Hadjisavvas and P. C. Kelires, Physica E (Amsterdam) **38** 99 (2007).
[17] *Computer Simulation of Liquids* (Oxford University Press, Oxford, England, 1989).
[18] H. Ohta and S. Hamaguchi, J. Chem. Phys. **115**, 6679 (2001).
[19] T. Watanabe, D. Yamasaki, K. K. Tatsumura, and I. Ohdomari, Appl. Surf. Sci. **234**, 207 (2004).
[20] J. Samela, K. Nordlund, V. N. Popok, and E. E. B. Campbell, Phys. Rev. B **77**, 075309 (2008).
[21] K. Lieb and J. Keinonen, Contemp. Phys. **47**, 305 (2006).
[22] F. Djurabekova, C. Björkas, and K. Nordlund, J. Phys.: Conf. Ser. (to be published).
[23] D. R. Lide, *CRC Handbook of Chemistry and Physics*, 82 ed. (CRC, Boca Raton, FL, 2001).
[24] F. Wooten, K. Winer, and D. Weaire, Phys. Rev. Lett. **54**, 1392 (1985).
[25] S. von Alfthan, A. Kuronen, and K. Kaski, Phys. Rev. B **68**, 073203 (2003).
[26] S. Susman, K. J. Volin, D. G. Montague, and D. L. Price, Phys. Rev. B **43**, 11076 (1991).
[27] R. L. Mozzi and B. E. Warren, J. Appl. Crystallogr. **2**, 164 (1969).
[28] R. Buczko, S. J. Pennycook, and S. T. Pantelides, Phys. Rev. Lett. **84**, 943 (2000).
[29] L. Khriachtchev, S. Novikov, and O. Kilpela, J. Appl. Phys. **87**, 7805 (2000).
[30] K. Nordlund, M. Ghaly, R. S. Averback, M. Caturla, T. Diaz de la Rubia, and J. Tarus, Phys. Rev. B **57**, 7556 (1998).
[31] Y. Q. Wang, R. Smirani, and G. G. Ross, Physica E (Amsterdam) **23**, 97 (2004).
[32] X. X. Wang, J. G. Zhang, L. Ding, B. W. Cheng, W. K. Ge, J. Z. Yu, and Q. M. Wang, Phys. Rev. B **72**, 195313 (2005).